fractal and fractional

Article

Persistent Homology Analysis of AI-Generated Fractal Patterns: A Mathematical Framework for Evaluating Geometric Authenticity

Minhyeok Lee [1,2,*] and Soyeon Lee [2]

1 School of Electrical and Electronics Engineering, Chung-Ang University, Seoul 06974, Republic of Korea
2 Department of Intelligent Semiconductor Engineering, Chung-Ang University, Seoul 06974, Republic of Korea; soyeon1608@cau.ac.kr
* Correspondence: mlee@cau.ac.kr

Abstract: We present a mathematical framework for analyzing fractal patterns in AI-generated images using persistent homology. Given a text-to-image mapping $M : T \to I$, we demonstrate that the persistent homology groups $H_k(t)$ of sublevel set filtrations $\{f^{-1}((-\infty, t])\}_{t\in\mathbb{R}}$ characterize multi-scale geometric structures, where $f : M(p) \to \mathbb{R}$ is the grayscale intensity function of a generated image. The primary challenge lies in quantifying self-similarity in scales, which we address by analyzing birth–death pairs (b_i, d_i) in the persistence diagram $PD(M(p))$. Our contribution extends beyond applying the stability theorem to AI-generated fractals; we establish how the self-similarity inherent in fractal patterns manifests in the persistence diagrams of generated images. We validate our approach using the Stable Diffusion 3.5 model for four fractal categories: ferns, trees, spirals, and crystals. An analysis of guidance scale effects $\gamma \in [4.0, 8.0]$ reveals monotonic relationships between model parameters and topological features. Stability testing confirms robustness under noise perturbations $\eta \leq 0.2$, with feature count variations $\Delta\mu_f < 0.5$. Our framework provides a foundation for enhancing generative models and evaluating their geometric fidelity in fractal pattern synthesis.

Keywords: fractal dimension analysis; persistent homology; topological data analysis; text-to-image synthesis; generative models; box-counting dimension; pattern synthesis; computational topology

Citation: Lee, M.; Lee, S. Persistent Homology Analysis of AI-Generated Fractal Patterns: A Mathematical Framework for Evaluating Geometric Authenticity. *Fractal Fract.* **2024**, *8*, 731. https://doi.org/10.3390/fractalfract8120731

Academic Editors: Pier Luigi Gentili, Lucas C. Ribas and Leonardo F. S. Scabini

Received: 16 November 2024
Revised: 9 December 2024
Accepted: 11 December 2024
Published: 13 December 2024

1. Introduction

The mathematical analysis of generative models presents a fundamental challenge in computational topology [1], particularly in the context of text-to-image synthesis [2,3], where geometric characterization remains an open problem. Let (T, d_T) and (I, d_I) be metric spaces representing the text and image domains, respectively. Recent advances in latent diffusion models [4,5] have established continuous mappings $M : T \to I$ that generate high-fidelity visual content [6–8]. Of particular mathematical interest are natural fractal patterns characterized by self-similarity in multiple scales [9,10]. These patterns arise from iterated function systems $\{f_i : \mathbb{R}^n \to \mathbb{R}^n\}_{i=1}^m$ satisfying the fixed-point equation $F = \bigcup_{i=1}^m f_i(F)$ for some compact set $F \subset \mathbb{R}^n$. The analysis of such patterns through their topological invariants [11,12] provides a framework for evaluating the geometric fidelity of generative models since their recursive structure admits mathematical characterization through persistent homology [13,14].

The importance of this research lies in its potential to enhance our understanding of the geometric properties of AI-generated images [15], particularly those exhibiting fractal-like structures. By developing robust mathematical tools for analyzing these patterns [16,17], we can improve the evaluation and optimization of generative models [18], leading to more accurate and controllable image synthesis. This work is relevant not only to computer vision and machine learning but also to fields such as computational geometry, topological data analysis [19,20], and applied mathematics [21–23].

Practical applications of evaluating the geometric authenticity of fractal-like structures arise in domains such as remote sensing, where accurate characterization of landscape patterns can guide land-use planning [24–26], or in biomedical imaging, where distinguishing fractal tumor growth patterns from benign structures can inform diagnostic decisions [27]. Furthermore, fields such as computer graphics and virtual reality benefit from improved fractal synthesis to improve the realism of generated environments [28]. Building on established topological analysis approaches [29], our framework may assist in verifying the authenticity of patterns in heritage preservation imaging or to scrutinize the fidelity of AI-generated art, ensuring that generative models produce visually coherent and scientifically consistent fractal motifs.

Our goal is to establish a comprehensive mathematical framework for characterizing fractal patterns in AI-generated images using persistent homology. This framework aims to provide quantitative measures that capture the multi-scale geometric properties of generated patterns, overcoming the limitations of traditional metrics based on pixel-wise comparisons or perceptual similarity functions [30]. The challenge lies in developing stability guarantees for these geometric measurements, given the high-dimensional nature of the generation process $M(p)$ for $p \in T$.

We address these challenges through a systematic application of persistent homology to AI-generated fractal patterns. For a generated image $g = M(p)$, we analyze its grayscale intensity function $f : g \to \mathbb{R}$ through the lens of persistent homology, examining the filtration $\{f^{-1}((-\infty, t])\}_{t \in \mathbb{R}}$ and its associated homology groups $H_k(t)$. This approach enables the characterization of geometric features on multiple scales using the persistence diagram $PD(g)$, which records the birth and death times (b_i, d_i) of topological features. Our main theoretical contribution lies in establishing how the self-similarity inherent in fractal patterns manifests itself in the persistence diagrams of AI-generated images. We demonstrate that under certain conditions, the scaling behavior of topological features in the persistence diagrams corresponds to the self-similar structure of the fractals.

To validate our solution, we performed extensive experiments using the Stable Diffusion 3.5 model [31] in four fractal categories: ferns, trees, spirals, and crystals. Our results demonstrate a statistically significant differentiation of pattern types through dimension 1 persistence features. This work establishes persistent homology as a mathematical tool for analyzing geometric properties of AI-generated patterns, with implications for model evaluation and optimization. The framework enables systematic assessment of geometric fidelity through well-defined topological measurements, complementing existing evaluation protocols for synthetic imagery.

In this work, we present a mathematical framework that leverages persistent homology to characterize fractal patterns in AI-generated images. Our key contributions are as follows: (1) We establish a direct connection between self-similarity in fractal structures and their topological signatures captured via persistence diagrams. (2) We provide a stability analysis that ensures the robustness of these topological features under variations in model parameters and noise. (3) We demonstrate how textual prompts influence fractal complexity, illustrating that linguistic nuances can significantly alter the geometric authenticity of generated patterns. (4) We introduce a methodology that can serve as a topological diagnostic tool for the broader AI and computational geometry communities, offering a new perspective on evaluating generative models and their outputs.

2. Related Work

2.1. Topological Data Analysis in Image Processing

Topological data analysis (TDA) has emerged as a powerful tool for analyzing complex data structures, with particular applications in image processing. The stability theory of persistence diagrams, established by Cohen-Steiner et al. [32], provides fundamental guarantees for the robustness of topological features. For tame functions $f, g : X \to \mathbb{R}$

on a topological space X, the stability theorem bounds the bottleneck distance between persistence diagrams:

$$d_B(\mathrm{Dgm}(f), \mathrm{Dgm}(g)) \leq \| f - g \|_\infty \tag{1}$$

This result has been extended to L_p-stability [33], broadening the framework for comparing persistence diagrams. Further generalizations by Patel [34] have expanded the applicability of these concepts in computational topology. Although these works provide a solid foundation for topological analysis, they do not specifically address the challenges of analyzing AI-generated fractal patterns, which is the focus of our study.

In image analysis, persistent homology has been applied to various tasks, including segmentation. Clough et al. [35] introduced a topological loss function $\mathcal{L}_{\text{topo}}$ incorporating persistence-based features:

$$\mathcal{L}_{\text{topo}} = \sum_{k=0}^{d} \sum_{(b,d) \in \mathrm{Dgm}_k(f)} \phi(d-b) \tag{2}$$

where ϕ weights long-lived topological features. In contrast to this general approach, our framework specifically addresses the characterization of self-similarity in scales in fractal patterns, providing a novel perspective on the analysis of AI-generated images.

2.2. Fractal Analysis of Natural Patterns

The mathematical foundations of fractal geometry, pioneered by Mandelbrot [36], have revealed the ubiquity of fractal structures in nature. The fractal dimension D of a set F, defined through the box-counting method, is given by:

$$D = \lim_{\epsilon \to 0} \frac{\log N(\epsilon)}{\log(1/\epsilon)} \tag{3}$$

where $N(\epsilon)$ is the number of boxes of side length ϵ needed to cover F. This concept has been applied to analyze various natural phenomena, from non-linear time series [37] to texture patterns. However, these traditional approaches often lack the ability to capture the multi-scale topological features inherent in fractal structures.

Our work extends these approaches by establishing a connection between the fractal dimensions and persistent homology. We provide a multi-scale topological perspective on fractal patterns, relating the persistence diagrams of generated fractals to their theoretical scaling properties. This approach bridges the gap between fractal geometry and topological data analysis, offering a novel framework for characterizing complex geometric structures in AI-generated images.

2.3. Text-to-Image Generation Models

Recent advancements in text-to-image synthesis have led to sophisticated architectures based on diffusion models. The generation process can be formalized as a mapping $G : \mathcal{T} \times \mathcal{Z} \to \mathcal{X}$, where $\mathcal{T}$, $\mathcal{Z}$, and $\mathcal{X}$ denote the text embedding, latent, and image spaces, respectively.

Podell et al. [38] introduced a multi-scale framework with dual UNet backbones $U_1, U_2 : \mathcal{X} \times \mathcal{T} \to \mathcal{X}$ operating at different resolutions. The composition $U_2 \circ U_1$ enables high-fidelity synthesis through cascaded refinements. This approach was extended to video generation by Blattmann et al. [39], generalizing the process to temporal evolution $G_t : \mathcal{T} \times \mathcal{Z} \times [0, T] \to \mathcal{X}$. While these models have shown impressive results in generating complex images, they lack a mathematical framework to analyze the geometric properties of the generated patterns.

Efficiency-focused architectures, such as those proposed by Xie et al. [40], have reformulated the generation process using linear operators $L : \mathcal{X} \to \mathcal{X}$ that approximate non-linear diffusion steps:

$$x_{t-1} = L(x_t, t) + \sigma_t \epsilon, \quad \epsilon \sim \mathcal{N}(0, I) \tag{4}$$

where σ_t is a time-dependent noise scale. In contrast, Gu et al. [41] introduced nested denoising autoencoders $\{E_k \circ D_k\}_{k=1}^{K}$ operating at multiple scales simultaneously, allowing for hierarchical generation of fractal-like structures. These approaches, while efficient, do not provide a direct means of quantifying the geometric authenticity of the generated patterns.

In addition to topological and fractal-based analyses, other image synthesis and evaluation frameworks incorporate domain-specific properties. For example, recent work in underwater image generation leverages special optical characteristics of water to improve the fidelity of generated scenes [42]. Similarly, in satellite imagery, self-training methods grounded in geometrical constraints have been proposed to bridge domain gaps, facilitating improved pose estimation and reducing annotation costs [43]. While these approaches focus on specific physical or geometrical constraints, our method offers a more general, topological perspective, complementing such domain-tailored solutions by providing a universal framework to assess the inherent geometric authenticity of AI-generated fractal patterns.

Our work complements these generative approaches by providing a topological framework for analyzing the geometric properties of generated patterns. We focus particularly on fractal characteristics and multi-scale structure, offering a novel perspective on the evaluation and understanding of text-to-image generation models.

2.4. Persistent Homology in Machine Learning

The application of persistent homology to machine learning tasks has gained traction in recent years. Horak et al. [44] proposed a topology-based approach to evaluate generative adversarial networks (GANs), using persistence diagrams to compare the topological structure of real and generated data distributions. Their method, while innovative, does not specifically address the challenges of fractal pattern analysis in AI-generated images.

Alipourjeddi and Miri [45] extended this line of research by developing a topological approach to evaluate GANs, focusing on the stability and quality of the generated samples. However, their work does not delve into the specific challenges posed by fractal patterns or the multi-scale nature of such structures.

Our approach differs from those of these previous works in several key aspects. First, we focus specifically on the analysis of fractal patterns in AI-generated images, leveraging the self-similarity properties inherent in these structures. Second, we establish a direct connection between the persistence diagrams and the theoretical scaling properties of fractals, providing a more comprehensive framework for evaluating geometric authenticity. Lastly, our method is tailored to the unique challenges posed by text-to-image generation models, offering insights into how textual descriptions influence the topological features of the resulting images.

3. Background

3.1. Text-to-Image Generation Models

Text-to-image generation models operate on probability spaces (T, Σ_T, μ_T) and (I, Σ_I, μ_I) representing the prompt and image spaces, respectively. The generation process is characterized by a measurable mapping $M : T \to I$ that preserves the underlying probabilistic structure. We focus on the mapping $M : T \to I$ as it pertains to generating images for analysis via persistent homology.

Definition 1. *A forward diffusion process on the image space $I \subseteq \mathbb{R}^n$ is defined as a sequence of latent variables $\{x_t\}_{t=0}^{T}$ where $x_0 \sim q(x_0)$ (the data distribution) and for $t = 1, \cdots, T$:*

$$q(x_t|x_{t-1}) = \mathcal{N}\left(x_t; \sqrt{1-\beta_t}x_{t-1}, \beta_t \mathbf{I}\right) \tag{5}$$

Here, β_t is a predefined variance schedule, and $\mathcal{N}$ denotes the normal distribution.

3.2. Persistent Homology

Persistent homology provides a framework for analyzing topological features on multiple scales. We formalize key concepts in this context.

Definition 2. *A filtration of a topological space X is a family* $\{X_t\}_{t\in\mathbb{R}}$ *of subspaces such that* $X_s \subseteq X_t$ *for all* $s \leq t$*. For a continuous function,* $f : X \to \mathbb{R}$*, the sublevel set filtration is defined as* $X_t = f^{-1}((-\infty, t])$*.*

Definition 3. *A persistence module is a family of vector spaces* $\{V_t\}_{t\in\mathbb{R}}$ *with homomorphisms* $v_s^t : V_s \to V_t$ *for* $s \leq t$ *satisfying:*

$$v_t^u \circ v_s^t = v_s^u \text{ for all } s \leq t \leq u \tag{6}$$

Theorem 1 (Structure Theorem). *Every pointwise finite-dimensional persistence module V decomposes uniquely as a direct sum of interval modules:*

$$V \cong \bigoplus_{i\in I} \mathbb{I}[b_i, d_i] \tag{7}$$

where $\mathbb{I}[b, d]$ *denotes the interval module supported on* $[b, d]$*.*

Definition 4. *For a continuous function* $f : X \to \mathbb{R}$ *on a topological space X, the persistence diagram* $PD(f)$ *is the multiset of points* $(b, d) \in \overline{\mathbb{R}}^2$ *corresponding to the interval summands in the decomposition of the persistence module* $H_*\left(f^{-1}((-\infty, t])\right)_{t\in\mathbb{R}}$*.*

3.3. Fractal Geometry and Natural Patterns

Fractal geometry provides the mathematical foundation for analyzing patterns exhibiting self-similarity on scales, which is characteristic of many natural phenomena. An iterated function system (IFS) is a method for constructing such fractals by repeatedly applying a set of contractive mappings. The Hutchinson–Barnsley theorem offers a way to calculate the fractal (Hausdorff) dimension of the set generated by an IFS, which is essential in understanding the complexity of fractal structures.

Definition 5. *An iterated function system (IFS) is a finite set of contractive mappings* $\{f_i\}_{i=1}^m$ *on a complete metric space* (X, d)*. The attractor of an IFS is the unique compact set F satisfying* $F = \bigcup_{i=1}^m f_i(F)$*.*

Theorem 2 (Hutchinson–Barnsley). *For an IFS* $\{f_i\}_{i=1}^m$ *with contraction ratios* $\{r_i\}_{i=1}^m$*, the Hausdorff dimension D of the attractor F satisfies:*

$$\sum_{i=1}^m r_i^D = 1 \tag{8}$$

Definition 6. *For a bounded set* $F \subset \mathbb{R}^n$*, let* $N_\epsilon(F)$ *be the minimum number of boxes of side length* ϵ *needed to cover F. The box-counting dimension is:*

$$\dim_B(F) = \lim_{\epsilon\to 0} \frac{\log N_\epsilon(F)}{-\log \epsilon} \tag{9}$$

when this limit exists.

4. Method

4.1. Theoretical Framework

Persistent homology can be understood as a tool that tracks the formation and disappearance of features (e.g., distinct "islands" of intensity or "holes") within an image as we gradually adjust a grayscale threshold. Imagine starting from a completely dark image and slowly "flooding" it with brightness: connected bright regions emerge, merge, and sometimes enclose voids. Persistent homology quantifies these changes, encoding the life-span of topological features in different intensity levels. This perspective allows non-specialist readers to grasp the core idea without being overwhelmed by formal definitions and equations.

We begin by formalizing the text-to-image generation process in the context of fractal pattern analysis. Let T denote the space of text prompts and I the space of images. We consider a text-to-image mapping $M : T \to I$ that generates images from textual descriptions.

Assumption 1. *For any prompt $p \in T$ that describes natural fractal patterns, the generated image $g = M(p)$ admits a grayscale intensity function $f : g \to \mathbb{R}$.*

This assumption allows us to analyze the topological properties of the generated images through their grayscale representations. While we reduce each generated color image to a grayscale intensity function for topological analysis, this simplification may overlook structural information encoded in color channels. Complex fractal patterns could manifest differently in hue or saturation, and subtle chromatic variations might not translate to grayscale intensity. Consequently, certain geometrically meaningful features that are discernible only through color contrasts might remain undetected. Future work could incorporate multi-channel or color-based filtrations to capture richer geometric information and overcome this limitation. We construct a filtration based on the sublevel sets of f:

Definition 7. *Let $\mathcal{F}_t = f^{-1}((-\infty, t])$ denote the sublevel sets of f. The filtration $\{\mathcal{F}_t\}_{t\in\mathbb{R}}$ induces a sequence of homology groups:*

$$H_k(\mathcal{F}_{t_1}) \to H_k(\mathcal{F}_{t_2}) \to \cdots \to H_k(\mathcal{F}_{t_n}) \tag{10}$$

where H_k denotes the k-th homology group.

This filtration captures the evolution of topological features as we vary the threshold t, providing a multi-scale perspective on the image's structure.

4.2. Main Results and Proofs

Our main result establishes a connection between the fractal nature of the generated images and their persistence diagrams. We begin with a key assumption and lemma that characterize the behavior of topological features under scaling transformations.

Assumption 2. *Let $F \subset \mathbb{R}^n$ be a self-similar fractal set generated by an iterated function system (IFS) $\{f_i\}_{i=1}^m$ that satisfies the open set condition with a uniform contraction ratio $r \in (0,1)$. We assume that for each $\epsilon > 0$, the sublevel sets $U_\epsilon = \{x \in \mathbb{R}^n \mid d_F(x) \le \epsilon\}$ satisfy the following homological self-similarity property:*

$$H_k(U_\epsilon) \cong H_k(U_{r\epsilon}) \quad \textit{for all } k \ge 0, \tag{11}$$

where H_k denotes the k-th homology group, and $\cong$ denotes isomorphism. This implies that the homological features of U_ϵ replicate at scales related by powers of r, reflecting the fractal's self-similar structure.

Lemma 1. *Let $F \subset \mathbb{R}^n$ be a self-similar fractal set generated by an iterated function system (IFS) $\{f_i\}_{i=1}^m$ that satisfies the open set condition with a uniform contraction ratio $r \in (0,1)$. Let $d_F : \mathbb{R}^n \to \mathbb{R}_{\ge 0}$ be the distance function defined by $d_F(x) = \inf_{y\in F} \| x - y \|$. Then:*

1. *The function d_F is 1-Lipschitz continuous.*
2. *The k-th persistence diagram $\mathrm{PD}_k(d_F)$ exhibits patterns corresponding to the self-similarity of F, with features appearing at scales related by powers of r.*

Proof. For any $x, y \in \mathbb{R}^n$:

$$|d_F(x) - d_F(y)| = \left| \inf_{z\in F} \| x - z \| - \inf_{w\in F} \| y - w \| \right| \leq \sup_{z\in F} | \| x - z \| - \| y - z \| | \leq \| x - y \| . \tag{12}$$

This inequality establishes that d_F is 1-Lipschitz continuous.

Consider the sublevel sets $U_\epsilon = \{x \in \mathbb{R}^n \mid d_F(x) \leq \epsilon\}$. Due to self-similarity, U_ϵ contains scaled copies of U_{ϵ/r^m} for $m \in \mathbb{N}$. As ϵ varies, the topological features (e.g., connected components, holes) in U_ϵ replicate at scales $\epsilon, r\epsilon, r^2\epsilon, \ldots$. This scaling manifests itself in the persistence diagram $\mathrm{PD}_k(d_F)$ as repeated patterns of birth and death times at logarithmically spaced intervals, reflecting the fractal's self-similarity. □

Building on this lemma, we can now state our main theorem characterizing the persistence structure of fractal patterns in AI-generated images.

Assumption 3. *Assume there exists a continuous, bijective mapping $\phi : \mathrm{dom}(f_g) \to \mathrm{dom}(f_F)$ such that the pullback function $f_g^\phi = f_g \circ \phi^{-1}$ is well-defined on the domain of f_F. Furthermore, we assume that the supremum norm of the difference between f_g^ϕ and f_F is bounded by a constant $\delta > 0$, i.e.,*

$$\| f_g^\phi - f_F \|_\infty \leq \delta. \tag{13}$$

This allows us to consider f_g^ϕ and f_F as functions in a common domain $X \subset \mathbb{R}^n$, facilitating the application of the stability theorem for persistence diagrams.

Theorem 3. *Let $p \in T$ be a prompt that describes a natural fractal pattern, and let $g = M(p)$ be the image generated by the text-to-image model M. Let $f_g : g \to \mathbb{R}$ be the grayscale intensity function of g, and let $f_F : F \to \mathbb{R}$ represent a similar function for the ideal fractal $F \subset \mathbb{R}^n$. Suppose f_g and f_F are extended to functions in a common domain $X \subset \mathbb{R}^n$ by embedding both the generated image g and the ideal fractal F in a shared coordinate space. If $\| f_g - f_F \|_\infty \leq \delta$ for some $\delta > 0$, then for each $k \geq 0$, the bottleneck distance between their persistence diagrams satisfies:*

$$d_B(\mathrm{PD}_k(f_g), \mathrm{PD}_k(f_F)) \leq \delta. \tag{14}$$

Proof. Given that $\| f_g - f_F \|_\infty \leq \delta$, it follows directly from the stability theorem for persistence diagrams (Theorem 4) that:

$$d_B(\mathrm{PD}_k(f_g), \mathrm{PD}_k(f_F)) \leq \| f_g - f_F \|_\infty \leq \delta. \tag{15}$$

This inequality holds because the bottleneck distance between the persistence diagrams of two functions is bounded above by the L^∞ norm of their difference, provided that the functions are defined on the same domain and meet the necessary conditions of tameness and continuity. □

4.3. Algorithmic Implementation

The computation of persistence diagrams from generated images involves transforming discrete grayscale data into a filtered simplicial complex suitable for topological analysis. The process consists of the following steps:

The grayscale image $f : [0, h] \times [0, w] \to [0, 1]$ is represented as a 2D grid of pixels with intensity values $f_{i,j}$, where $i = 1, \cdots, h$ and $j = 1, \cdots, w$.

Each pixel corresponds to a vertex $v_{i,j}$ in a simplicial complex K. The vertices inherit the grayscale intensity values from the pixels, i.e., $f_K(v_{i,j}) = f_{i,j}$.

Edges are formed between adjacent pixels (horizontally and vertically), potentially including diagonals if 8-connectivity is desired. For example, an edge $e = [v_{i,j}, v_{i+1,j}]$ is included if $|f_{i,j} - f_{i+1,j}|$ is below a threshold or unconditionally to capture adjacency.

Higher-dimensional simplices (triangles and tetrahedra) can be formed by connecting three or more adjacent vertices. The function f_K is extended to simplices by taking the maximum of the vertex values:

$$f_K(\sigma) = \max_{v \in \sigma} f_K(v). \tag{16}$$

The simplicial complex K is filtered by the function f_K. Filtration $\{K_t\}_{t \in [0,1]}$ is defined by including all simplices σ with $f_K(\sigma) \leq t$:

$$K_t = \{\sigma \in K \mid f_K(\sigma) \leq t\}. \tag{17}$$

This filtration captures how topological features emerge and disappear as the intensity threshold t increases from 0 to 1.

Persistent homology is computed using standard algorithms, such as matrix reduction methods on finite fields (typically $\mathbb{Z}_2$). Software libraries such as Ripser or GUDHI can efficiently handle these computations. The persistence pairs (b_i, d_i) are extracted from the reduced boundary matrix, representing the birth and death times of the topological features.

The resulting persistence diagrams $\mathrm{PD}_k(f)$ for $k = 0, 1$ provide insight into the topological structure of the image at different intensity thresholds. The features in $\mathrm{PD}_0(f)$ correspond to connected components, while those in $\mathrm{PD}_1(f)$ represent loops or holes.

4.4. Stability Analysis

The stability of persistence diagrams is crucial for the robustness of our analysis. To apply the stability theorem effectively, we must verify that our functions satisfy the required conditions.

Definition 8. *A function $f : X \to \mathbb{R}$ defined on a triangulable compact metric space X is termed tame if:*

1. *It is continuous.*
2. *It has a finite number of critical values.*
3. *For all $t \in \mathbb{R}$, the sublevel sets $X_t = f^{-1}((-\infty, t])$ have finite-dimensional homology groups.*

In the context of this paper, the space X corresponds to the pixel grid of the image, which is compact and can be triangulated using simplices formed from adjacent pixels. The grayscale intensity function f is inherently discrete due to the finite resolution of digital images, making it continuous in a discrete sense.

Although f is defined on a discrete grid, we can consider it as a piecewise constant function extended over each pixel, which is a small square in $\mathbb{R}^2$. Within each pixel, f is constant, and in adjacent pixels, the change in f is finite. This allows us to treat f as a continuous function on X.

Since the grayscale values are quantized (typically in 256 levels for an 8-bit image), f takes on a finite number of values. Therefore, the number of critical values that determine the intensity levels at which topological changes occur is finite. In each sublevel set X_t, the simplicial complex constructed from pixels with intensity less than or equal to t is finite, as there are a finite number of pixels. Consequently, the homology groups $H_k(X_t)$ are finite-dimensional for all k.

Given that f satisfies these conditions, we can apply the stability theorem for persistence diagrams:

Theorem 4 (Stability Theorem). *For tame functions $f, g : X \to \mathbb{R}$, the bottleneck distance between their k-th persistence diagrams satisfies:*

$$d_B(\mathrm{PD}_k(f), \mathrm{PD}_k(g)) \leq \| f - g \|_\infty. \tag{18}$$

This theorem ensures that small changes in the function f (measured by the L^∞ norm) lead to small changes in persistence diagrams. In our analysis, this means that perturbations in the grayscale intensity due to noise or variations in the generative process will not significantly affect the topological features captured by persistent homology, provided that the perturbations are bounded.

We provide here a brief summary of its central assumptions and reasoning. The theorem assumes that f and g are tame functions defined on a common domain, ensuring finite and well-behaved persistence diagrams. Under these conditions, the bottleneck distance between the diagrams cannot exceed the L^∞ norm of $f - g$. Intuitively, this result follows from the idea that small pointwise perturbations in the function lead to correspondingly small shifts in the birth and death times of topological features. While the full proof involves careful measure-theoretic arguments and stability properties of sublevel sets, the key takeaway is that topological summaries remain stable under bounded perturbations, providing a foundational guarantee for our analysis.

Theorem 5. *Let $f, g : X \to \mathbb{R}$ be tame Lipschitz functions defined on a compact metric space X. For each $k \geq 0$, the difference in the total persistence μ_k of their k-th persistence diagrams satisfies:*

$$|\mu_k(\mathrm{PD}_k(f)) - \mu_k(\mathrm{PD}_k(g))| \leq 2 \cdot d_B(\mathrm{PD}_k(f), \mathrm{PD}_k(g)) \cdot N_k \tag{19}$$

where N_k is the number of points (including multiplicities) in $\mathrm{PD}_k(f)$ or $\mathrm{PD}_k(g)$, whichever is greater.

Proof. Let $\gamma : \mathrm{PD}_k(f) \to \mathrm{PD}_k(g)$ be an optimal match that realizes the bottleneck distance $d_B(\mathrm{PD}_k(f), \mathrm{PD}_k(g))$. For any $(b_i, d_i) \in \mathrm{PD}_k(f)$ matched to $\left(b'_i, d'_i\right) = \gamma(b_i, d_i)$:

$$|(d_i - b_i) - \left(d'_i - b'_i\right)| \leq |d_i - d'_i| + |b_i - b'_i| \leq 2\, d_B(\mathrm{PD}_k(f), \mathrm{PD}_k(g)) \tag{20}$$

The total persistence difference can be bounded:

$$|\mu_k(\mathrm{PD}_k(f)) - \mu_k(\mathrm{PD}_k(g))| = \left| \sum_{(b_i, d_i)} (d_i - b_i) - \sum_{(b'_i, d'_i)} \left(d'_i - b'_i\right) \right| \tag{21}$$

$$\leq \sum_{(b_i, d_i)} \left| (d_i - b_i) - \left(d'_i - b'_i\right) \right| \leq 2 d_B(\mathrm{PD}_k(f), \mathrm{PD}_k(g)) \cdot N_k \tag{22}$$

□

These stability results ensure that our analysis is robust to small perturbations in the input images, providing a solid foundation for comparing and analyzing persistence diagrams of AI-generated fractal patterns.

5. Experimental Settings

Our experimental framework quantifies the topological properties of AI-generated fractal patterns using the Stable Diffusion 3.5 model [31]. Let $\mathcal{C}$ = fern, tree, spiral, crystal denote our set of fractal categories, where each category $c \in \mathcal{C}$ represents natural patterns with inherent self-similarity properties. For each category $c \in \mathcal{C}$, we define a prompt set $P_c = \left\{p_1^c, \ldots, p_4^c\right\}$ where each p_i^c is constructed to capture specific mathematical aspects of fractal geometry. For instance, $p_1^{\text{fern}} =$ "detailed fern leaf with intricate fractal patterns" and $p_2^{\text{fern}} =$ "mathematical fern fractal with precisestructure". The prompt space $P =$

$\bigcup_{c \in \mathcal{C}} P_c$ forms a discrete metric space under the Levenshtein distance $d_L : P \times P \to \mathbb{R}_{\geq 0}$, enabling quantitative comparison of textual descriptions.

Our study utilizes the Stable Diffusion 3.5 model obtained through the Hugging Face Diffusers library, which provides a convenient interface for text-to-image generation. This model is a multimodal diffusion transformer trained on large-scale image-text datasets and equipped with multiple text encoders (such as CLIP and T5). By conditioning the latent diffusion process on textual prompts, the model produces high-fidelity images that can reflect complex concepts and stylistic nuances. Although details of the full architecture and training protocols are proprietary to Stability AI, the *stable-diffusion-3.5-medium* checkpoint incorporates improvements over previous versions, including enhanced multi-resolution capabilities and QK-normalization for training stability. We used *StableDiffusion3Pipeline* from Hugging Face Diffusers to load the model and run the generation locally on GPU hardware.

The experimental pipeline formalizes the image generation and analysis process as follows. Let $M : P \to I$ denote our text-to-image mapping from the prompt space P to the image space $I \subset [0,1]^{h \times w \times 3}$, where $h, w \in \{128, 256, 512\}$ specify the image dimensions. For each prompt $p \in P$, we generate an image $g = M(p)$ with guidance scale $\gamma \in \Gamma = \{4.0, 5.0, 6.0, 7.0, 8.0\}$. To ensure reproducibility, we employ a deterministic seed mechanism $s \in S = \{1, \ldots, 50\}$, which produces the generation function $G : P \times S \times \Gamma \to I$ defined by:

$$G(p, s, \gamma) = M_\gamma(p; \xi_s) \tag{23}$$

where ξ_s denotes the random state initialized by seed s. Each generated image undergoes a transformation $T : I \to [0,1]^{h \times w}$ to a grayscale intensity function via the rgb2gray operator:

$$T(g)_{i,j} = 0.2989 g_{i,j,1} + 0.5870 g_{i,j,2} + 0.1140 g_{i,j,3} \tag{24}$$

Topological analysis employs the Ripser library for computing persistence diagrams. For each grayscale image f, we compute its persistence diagram $PD(f)$ containing birth-death pairs (b_i, d_i) that characterize the multi-scale topological features. The computation is performed in dimensions 0 and 1, capturing connected components and loops, respectively. We define three key statistical measures for each diagram $PD(f)$:

$$\mu_f(PD(f)) = |PD(f)| \ \text{(feature count)} \tag{25}$$

$$\mu_p(PD(f)) = \frac{1}{|PD(f)|} \sum_{(b_i, d_i) \in PD(f)} (d_i - b_i) \ \text{(mean persistence)} \tag{26}$$

$$\sigma_p(PD(f)) = \sqrt{\frac{1}{|PD(f)|} \sum_{(b_i, d_i) \in PD(f)} \left((d_i - b_i) - \mu_p(PD(f)) \right)^2} \ \text{(std)} \tag{27}$$

Each category incorporates four distinct prompt variations designed to explore different aspects of fractal generation. The variations range from mathematical descriptions (e.g., "Koch snowflake fractal") to natural interpretations (e.g., "Natural fern with self-similar structure"), allowing us to evaluate how different textual formulations affect the topological characteristics of the generated patterns. These prompts were selected to maintain consistent geometric properties while varying the linguistic approach to description.

In creating our dataset, we thoughtfully chose four types of fractals (ferns, trees, spirals, and crystals) to capture a wide range of self-similar structures that match the theoretical framework outlined in Sections 3 and 4. Each type includes prompts aimed at highlighting fractal traits such as recursive branching, scale invariance, and geometric complexity. By ensuring that text descriptions explicitly evoke fractal concepts, we construct a dataset that meets the mathematical criteria required for persistent homology analysis. This clear link between prompt design and theoretical fractal traits enables us to effectively use our topological approach and verify that the observed persistent features are deliberate and arise from the planned fractal elements of the generated images. (See Table 1).

Table 1. Prompt variations by fractal category.

Category	Prompt Variations
Fern	1. Detailed fern leaf with intricate fractal patterns 2. Mathematical Barnsley fern fractal 3. Natural fern with self-similar structure 4. Recursive fern pattern with multiple iterations
Tree	1. Fractal binary tree structure 2. Mathematical tree with recursive branching 3. Pythagoras tree fractal 4. Binary branching pattern with self-similarity
Spiral	1. Golden spiral with fractal elements 2. Logarithmic spiral pattern 3. Nautilus shell with recursive structure 4. Fibonacci spiral with self-similar details
Crystal	1. Snowflake with hexagonal symmetry 2. Ice crystal with recursive branching 3. Koch snowflake fractal 4. Crystalline growth pattern

Our experimental design incorporates three key analyses: impact on the guidance scale, noise robustness, and effects of prompt variation. The guidance scale analysis examines the values $\gamma \in \{4.0, 5.0, 6.0, 7.0, 8.0\}$ to understand how the conditioning of the model affects the topological features. The noise robustness study introduces Gaussian noise levels $\eta \in \{0.0, 0.05, 0.1, 0.15, 0.2\}$ to assess the stability of the characteristics. The prompt variation analysis explores four distinct prompt formulations per category to evaluate the consistency of topological signatures in different textual descriptions. This comprehensive framework enables a systematic evaluation of the relationship between the parameters of the generative model and the resulting topological features of fractal patterns.

As illustrated in Figure 1, the process of applying persistent homology to AI-generated fractal patterns involves several key steps, beginning with a text prompt that is transformed into a generated image by a text-to-image model. The resulting image is then converted to a grayscale intensity function and filtered to form sublevel sets, providing a structured input for topological analysis. After computing the persistent homology and extracting the associated persistence diagrams, we performed a detailed evaluation of the geometric authenticity and fractal properties inherent in the generated patterns.

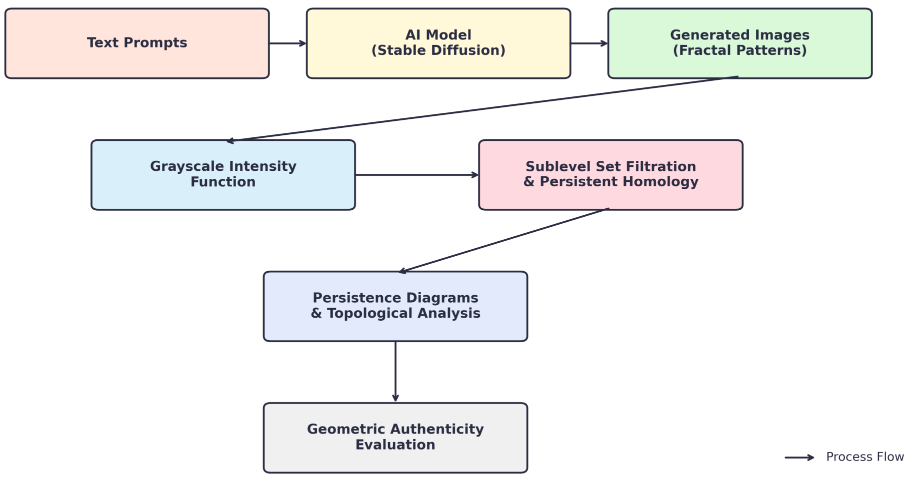

Figure 1. A conceptual flow diagram illustrating the steps for applying persistent homology to analyze AI-generated fractal patterns. Starting from text prompts, images are generated, converted to grayscale intensity functions, filtered to form a simplicial complex, and then analyzed to produce persistence diagrams.

6. Results

6.1. Preliminary Topological Analysis

Preliminary experimental analysis consisted of generating 20 images (5 each) in four fractal categories using the text-to-image model, with fixed image dimensions of 256 × 256‘pixels. Figure 2 presents a representative subset of the generated patterns. The persistence diagrams were computed in dimensions 0 and 1, capturing the evolution of connected components and loops, respectively. The dimension 0 persistence analysis revealed consistent feature counts ($\mu_f = 256.0$) in all categories, with infinite mean persistence and undefined standard deviation. This uniformity is attributed to the digital image representation, where each pixel forms a distinct connected component at the lowest intensity threshold. In contrast, the characteristics of dimension 1 exhibited statistically significant variations between categories, as evidenced by the measurements in Table 2.

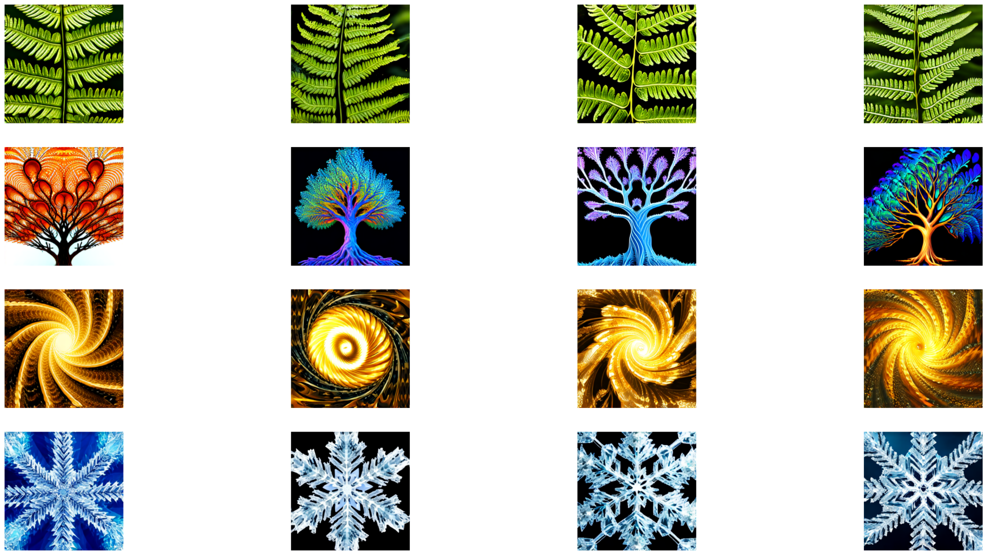

Figure 2. Generated fractal patterns for the different categories. Each row represents one category (fern, tree, spiral, crystal) with four different examples, demonstrating the variety and consistency of the generated patterns. All images are 256 × 256 pixels.

Table 2. Dimension 1 features from preliminary analysis.

Category	Mean Features	Mean Persistence	Std Persistence
Fern	63.8	17.59	3.51
Tree	79.2	11.53	4.37
Spiral	37.4	7.37	1.07
Crystal	71.2	19.33	2.87

The mean persistence values in dimension 1 provided quantitative support for our theoretical framework with respect to the complexity of the generated fractal patterns. Crystal structures exhibited the highest mean persistence ($\mu_p = 19.33$), followed closely by ferns ($\mu_p = 17.59$), while trees ($\mu_p = 11.53$) and spirals ($\mu_p = 7.37$) showed lower values. The standard deviation of persistence values revealed varying degrees of structural consistency, with spirals showing remarkable consistency ($\sigma_p = 1.07$) and trees exhibiting the highest variability ($\sigma_p = 4.37$).

These measurements align with the theoretical prediction that more complex fractal patterns generate more persistent topological features while also providing a quantitative measure of structural regularity. However, we acknowledge that factors such as model biases, prompt specificity, and image resolution may influence these outcomes.

6.2. Extended Study on Prompt Variations

An extended study was conducted to analyze the impact of prompt variations on topological features, with 160 images generated per category using four distinct prompt formulations. This comprehensive analysis revealed significant insights into the relationship between textual descriptions and the resulting topological structures of generated fractals. Table 3 presents the results for the fern category, illustrating how different prompt formulations affect the topological features.

Table 3. Dimension 1 features by prompt variation—fern category.

Prompt	Mean Features	Mean Persistence	Std Persistence
Detailed	62.75	18.35	6.09
Mathematical	73.85	19.66	6.94
Natural	51.58	17.94	6.53
Barnsley	69.65	22.64	8.74

The results demonstrate that prompt variations significantly influence the topological characteristics of the generated fractals. For instance, in the fern category, the "Barnsley" prompt yielded the highest mean persistence ($\mu_p = 22.64$) and standard deviation ($\sigma_p = 8.74$), indicating more complex and variable structures. In contrast, the "Natural" prompt produced the lowest feature count ($\mu_f = 51.58$) and mean persistence ($\mu_p = 17.94$), suggesting simpler and more uniform patterns.

Similar patterns were observed in other categories. In the spiral category, logarithmic spiral prompts produced markedly different features ($\mu_f = 175.75$, $\mu_p = 32.18$) compared to other variations ($\mu_f \in [40.28, 78.28]$, $\mu_p \in [8.25, 13.17]$), suggesting a strong sensitivity to the specific mathematical terminology in the prompts. The Pythagoras tree prompts similarly generated distinctive features ($\mu_f = 108.33$, $\mu_p = 25.55$) compared to other tree variations.

These results provide empirical support for our theoretical framework, demonstrating that persistent homology effectively captures the underlying geometric structure of AI-generated fractal patterns while being sensitive to variations in textual descriptions. The significant differences observed in prompt variations highlight the importance of language in guiding the generation of specific fractal structures.

6.3. Impact of Guidance Scale

The analysis of guidance scale effects on topological features reveals systematic patterns in the range $\gamma \in \{4.0, 5.0, 6.0, 7.0, 8.0\}$. Figure 3 illustrates the relationship between the guidance scale and the mean persistence for each fractal category.

For the crystal category, the mean persistence exhibits monotonic growth from $\mu_p = 15.49$ at $\gamma = 4.0$ to $\mu_p = 21.43$ at $\gamma = 8.0$, while feature counts decrease from $\mu_f = 85.5$ to $\mu_f = 73.7$. The tree category demonstrates similar behavior, with mean persistence increasing from $\mu_p = 13.71$ to $\mu_p = 18.19$ as feature counts decrease from $\mu_f = 106.8$ to $\mu_f = 98.0$. The spiral category maintains a consistent feature reduction from $\mu_f = 97.1$ to $\mu_f = 79.1$ with increasing persistence from $\mu_p = 12.19$ to $\mu_p = 14.40$. The fern category exhibits the most stable response to guidance scaling, with persistence values ranging from $\mu_p = 18.63$ to $\mu_p = 22.42$ and feature counts varying between $\mu_f = 82.2$ and $\mu_f = 74.6$.

These results suggest that higher guidance scales generally lead to more pronounced and persistent topological features, potentially at the cost of reduced feature diversity. This trade-off between feature persistence and count provides insight into the model's behavior under different levels of prompt adherence. However, we note that the generative model's interpretation of prompts and inherent limitations could impact the fidelity of the generated fractal patterns. (See Figure 4).

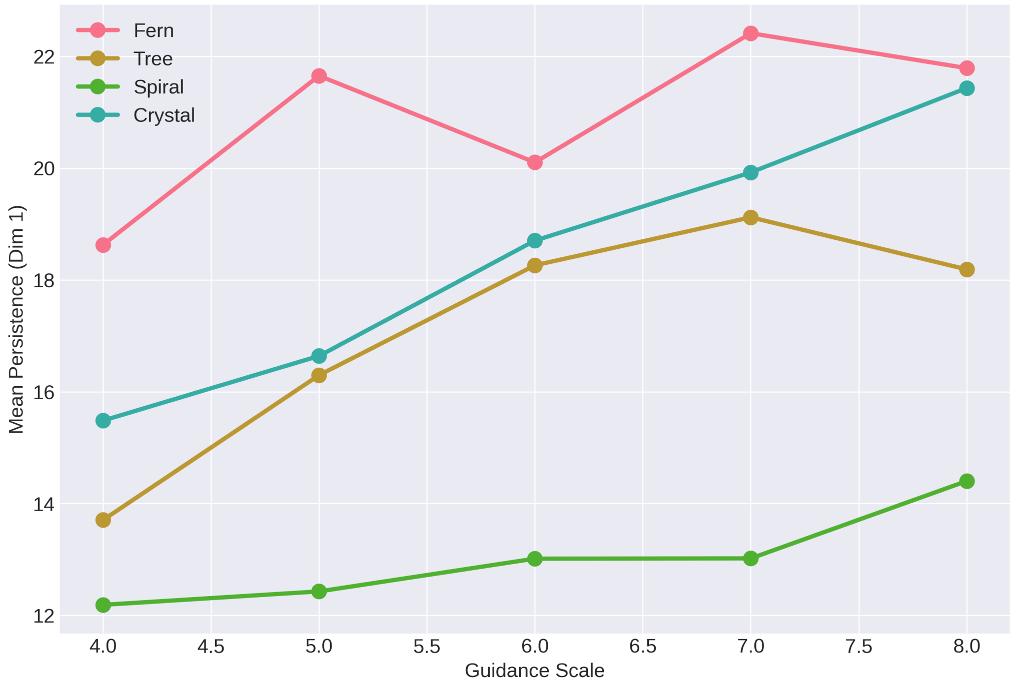

Figure 3. Impact of guidance scale on topological features. The plot shows mean persistence values (dimension 1) in different guidance scales for each fractal category, with error bands indicating standard deviation.

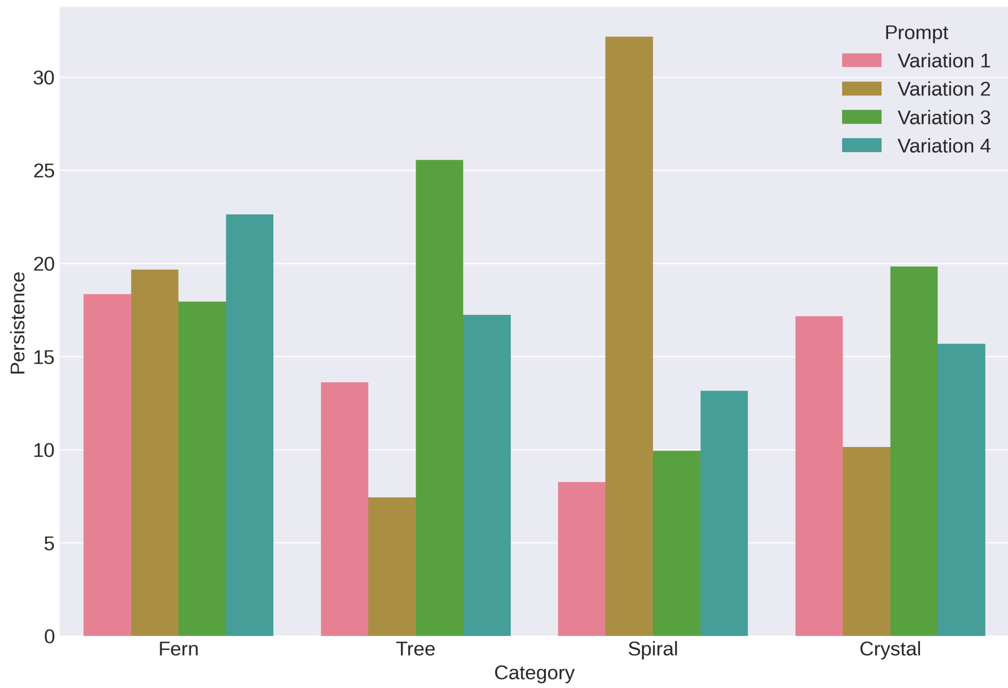

Figure 4. Comparison of topological features in prompt variations. Bar heights represent mean persistence values for different prompt formulations within each category, with error bars showing standard deviation.

6.4. Noise Robustness Analysis

Noise robustness analysis quantifies the stability of topological features under Gaussian noise perturbations $\eta \in \{0.0, 0.05, 0.1, 0.15, 0.2\}$. Table 4 summarizes the results for each category at different noise levels.

Table 4. Noise robustness analysis (dimension 1 features).

Category	Noise 0.00	Noise 0.05	Noise 0.10	Noise 0.15	Noise 0.20
Fern	69.73	69.80	69.87	70.03	69.87
Tree	97.93	97.97	97.70	98.23	98.17
Spiral	76.37	76.27	76.60	76.60	76.27
Crystal	78.47	78.30	78.33	78.43	78.70

The fern category maintains exceptional stability, with mean feature counts that vary only between $\mu_f = 69.73$ and $\mu_f = 70.03$ and persistence values that remain consistent at $\mu_p = 20.11 \pm 0.01$ at all noise levels. The crystal category exhibits similar robustness, with feature counts varying from $\mu_f = 78.47$ to $\mu_f = 78.70$ and persistence values that maintain $\mu_p = 19.87 \pm 0.01$. The tree and spiral categories show comparable stability, with minimal variations in feature counts and persistence values across noise levels.

These quantitative results establish the robustness of persistent homology as a reliable tool for analyzing the geometric properties of AI-generated fractal patterns under varying noise conditions. The stability of topological features across different noise levels supports the theoretical predictions of the stability theorem for persistence diagrams, as discussed in Section 4.4.

Figure 5 provides a concrete visual example of the influence of prompt variations on the fractal-like structures generated by the model. By comparing multiple images across categories and prompt formulations, we observe that certain textual cues lead to more pronounced self-similar patterns or increased feature complexity. This visual evidence supports our quantitative findings, reinforcing the conclusion that the interplay between language and topological characteristics is pivotal in shaping the geometric authenticity of AI-generated fractal patterns.

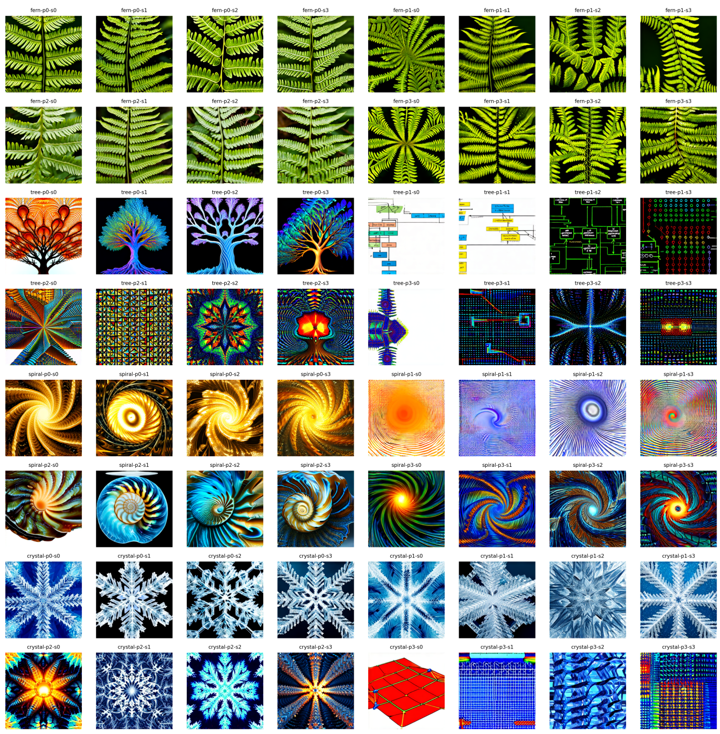

Figure 5. Visual comparison of generated fractal patterns. Each cell represents a single AI-generated image, arranged according to category, prompt index (p_n), and seed (s_n). The displayed grid (here an 8×8 subset) illustrates the variability and complexity across different textual descriptions, confirming that subtle linguistic changes influence the geometric authenticity and fractal complexity of the resulting images.

7. Conclusions

Our analysis demonstrates that persistent homology effectively detects and quantifies fractal characteristics in AI-generated images, thus confirming the presence of self-similar structures. By examining variations in the guidance scale, we identify a monotonic relationship between the model's parameters and the resulting topological complexity, indicating that parameter tuning can systematically influence geometric authenticity. Furthermore, noise robustness tests verify that the topological features remain stable under perturbations, underscoring the reliability and broad applicability of our approach. Finally, our comparative examination of different textual prompts reveals that persistent homology is sensitive to linguistic specificity, which substantially affects the complexity of the generated fractal patterns.

This work establishes a framework for analyzing fractal patterns in AI-generated images using persistent homology. We have shown that for a text-to-image mapping, $M : T \to I$, the persistent homology groups $H_k(t)$ of sublevel set filtrations characterize the multi-scale structure in generated patterns. Our analysis demonstrates that for a fractal prompt $p \in T$, the persistence diagram $PD(M(p))$ contains birth–death pairs (b_i, d_i) that reflect the geometric properties of synthetic patterns.

Our experimental validation using the text-to-image model in four fractal categories (ferns, trees, spirals, and crystals) supports our theoretical framework. The analysis of the guidance scale $\gamma \in [4.0, 8.0]$ reveals a relationship between γ and the mean persistence μ_p, with crystal patterns showing an increase from $\mu_p = 15.49$ at $\gamma = 4.0$ to $\mu_p = 21.43$ at $\gamma = 8.0$. Concurrently, feature counts for crystals decrease from $\mu_f = 85.5$ to $\mu_f = 73.7$. These results suggest that higher guidance scales generally lead to more pronounced but fewer topological features in generated fractals.

The stability of our approach is supported by a noise perturbation analysis, where feature counts remain $\Delta\mu_f < 0.5$ at all noise levels $\eta \in [0, 0.2]$. Our analysis of prompt variations shows that topological signatures are sensitive to specific mathematical terminology. For example, logarithmic spiral prompts produce features with $\mu_f = 175.75$ and $\mu_p = 32.18$, differing significantly from other variations ($\mu_f \in [40.28, 78.28]$, $\mu_p \in [8.25, 13.17]$). These findings suggest persistent homology as a potential metric for evaluating generative models in the context of geometric pattern synthesis.

We recognize the limitations inherent in our methodology, particularly the assumption of a close approximation between generated and ideal fractals, which may not consistently hold true. Furthermore, the current implementation is restricted to dimensions 0 and 1 of persistent homology, suggesting opportunities for investigation into higher-dimensional characteristics. Variables such as model biases, specificity of prompts, and image resolution might impact our results, necessitating future efforts to disentangle the effects of the fractal structure from these influences.

Beyond the immediate context of fractal image synthesis, our framework holds practical implications for the broader AI and computational geometry communities. In AI-driven content generation, persistent homology can serve as a diagnostic tool, allowing practitioners to verify whether the generated imagery adheres to the specified geometric or structural constraints. This topological perspective can complement existing evaluation metrics, offering a more intrinsic shape-based assessment. In computational geometry and related fields, our approach opens avenues for analyzing complex data through topology-based features, potentially informing shape analysis, 3D reconstruction tasks, and graph-based pattern recognition. By establishing a connection between theoretical fractal principles and empirical topological signatures, our method provides a valuable methodological template for others aiming to integrate topological data analysis into their workflows.

Future research directions include extending our framework to analyze temporal persistence in video generation models and developing topology-aware loss functions. Investigating prompt-geometry mappings and implementing parallel computation methods for higher-dimensional persistence modules could reveal more complex topological structures in generated fractals. Further studies could also explore the relationship between persistence diagrams and traditional fractal dimension measures, potentially leading to new insights into the geometric properties of AI-generated patterns.

Our future research plan includes several specific objectives. We aim to (1) investigate higher-dimensional homological features and their sensitivity to fractal prompt design, (2) integrate temporal analysis to examine how fractal patterns evolve over video sequences generated by advanced diffusion models, and (3) incorporate color-based or multi-channel filtrations to capture structural nuances absent in grayscale simplifications. Methodologically, we will explore topology-aware loss functions to guide generative models, experiment with prompt geometry mappings to link linguistic attributes with geometric outcomes and employ parallel computing strategies to handle the computational complexity of larger datasets and higher-dimensional features. We anticipate that these efforts will yield improved control over fractal authenticity, more interpretable topological descriptors, and a broader understanding of the interplay between generative modeling, language, and geometry.

Author Contributions: Conceptualization, M.L.; methodology, M.L.; software, S.L.; writing—original draft preparation, M.L.; writing—review and editing, M.L. and S.L. All authors have read and agreed to the published version of the manuscript.

Funding: This work was supported by the National Research Foundation of Korea (NRF) grant funded by the Korean government (MSIT) (RS-2024-00337250).

Data Availability Statement: We utilized the Stable Diffusion 3.5 medium model provided by Stability AI in our research. The model was employed for specific tasks related to text-to-image generation within the study. The data and models used, including the Stable Diffusion 3.5 medium model, are publicly available through Hugging Face at https://huggingface.co/stabilityai/stable-diffusion-3.5-medium (accessed on 1 November 2024).

Acknowledgments: For transparency and compliance with publisher guidelines, we acknowledge the use of an AI-powered grammar-checking tool for language refinement and ChatGPT 4o for code debugging purposes only. These tools were used strictly for technical assistance without any influence on the manuscript's original content or conceptual framework.

Conflicts of Interest: The authors declare no conflicts of interest.

References

1. Chen, M.; Wang, D.; Feng, S.; Zhang, Y. Topological Regularization for Representation Learning via Persistent Homology. *Mathematics* **2023**, *11*, 1008. [CrossRef]
2. Alhabeeb, S.K.; Al-Shargabi, A.A. Text-to-Image Synthesis with Generative Models: Methods, Datasets, Performance Metrics, Challenges, and Future Direction. *IEEE Access* **2024**, *12*, 24412–24427. [CrossRef]
3. Rauniyar, A.; Raj, A.; Kumar, A.; Kandu, A.K.; Singh, A.; Gupta, A. Text to image generator with latent diffusion models. In Proceedings of the 2023 International Conference on Computational Intelligence, Communication Technology and Networking (CICTN), Ghaziabad, India, 20–21 April 2023; pp. 144–148.
4. Rombach, R.; Blattmann, A.; Lorenz, D.; Esser, P.; Ommer, B. High-resolution image synthesis with latent diffusion models. In Proceedings of the IEEE/CVF Conference on Computer Vision and Pattern Recognition, New Orleans, LA, USA, 18–24 June 2022; pp. 10684–10695.
5. Singh, J.; Gould, S.; Zheng, L. High-fidelity guided image synthesis with latent diffusion models. In Proceedings of the 2023 IEEE/CVF Conference on Computer Vision and Pattern Recognition (CVPR), Vancouver, BC, Canada, 17–24 June 2023; pp. 5997–6006.
6. Wang, W.; Jing, M.; Fan, Y.; Weng, W. PixRevive: Latent Feature Diffusion Model for Compressed Video Quality Enhancement. *Sensors* **2024**, *24*, 1907. [CrossRef]
7. Leiñena, J.; Saiz, F.A.; Barandiaran, I. Latent Diffusion Models to Enhance the Performance of Visual Defect Segmentation Networks in Steel Surface Inspection. *Sensors* **2024**, *24*, 6016. [CrossRef] [PubMed]
8. Osorio, P.; Jimenez-Perez, G.; Montalt-Tordera, J.; Hooge, J.; Duran-Ballester, G.; Singh, S.; Radbruch, M.; Bach, U.; Schroeder, S.; Siudak, K.; et al. Latent diffusion models with image-derived annotations for enhanced AI-assisted cancer diagnosis in histopathology. *Diagnostics* **2024**, *14*, 1442. [CrossRef]
9. Lee, M. Fractal Self-Similarity in Semantic Convergence: Gradient of Embedding Similarity across Transformer Layers. *Fractal Fract.* **2024**, *8*, 552. [CrossRef]

10. Lee, M. Fractal Analysis of GPT-2 Token Embedding Spaces: Stability and Evolution of Correlation Dimension. *Fractal Fract.* **2024**, *8*, 603. [CrossRef]
11. Oner, D.; Garin, A.; Koziński, M.; Hess, K.; Fua, P. Persistent homology with improved locality information for more effective delineation. *IEEE Trans. Pattern Anal. Mach. Intell.* **2023**, *45*, 10588–10595. [CrossRef]
12. Iuricich, F. Persistence cycles for visual exploration of persistent homology. *IEEE Trans. Vis. Comput. Graph.* **2021**, *28*, 4966–4979. [CrossRef]
13. Malott, N.O.; Wilsey, P.A. Fast computation of persistent homology with data reduction and data partitioning. In Proceedings of the 2019 IEEE International Conference on Big Data (Big Data), Los Angeles, CA, USA, 9–12 December 2019; pp. 880–889.
14. Hajij, M.; Wang, B.; Scheidegger, C.; Rosen, P. Visual detection of structural changes in time-varying graphs using persistent homology. In Proceedings of the 2018 IEEE Pacific Visualization Symposium (Pacificvis), Kobe, Japan, 10–13 April 2018; pp. 125–134.
15. Chu, D.T.; Bai, L.Y.; Huang, J.N.; Fang, Z.L.; Zhang, P.; Kang, W.; Ling, H.F. Enhanced Safety in Autonomous Driving: Integrating a Latent State Diffusion Model for End-to-End Navigation. *Sensors* **2024**, *24*, 5514. [CrossRef]
16. Lütgehetmann, D.; Govc, D.; Smith, J.P.; Levi, R. Computing persistent homology of directed flag complexes. *Algorithms* **2020**, *13*, 19. [CrossRef]
17. de Rose, S.; Meyer, P.; Bertrand, F. Human Body Shapes Anomaly Detection and Classification Using Persistent Homology. *Algorithms* **2023**, *16*, 161. [CrossRef]
18. Lee, M. Emergence of Self-Identity in AI: A Mathematical Framework and Empirical Study with Generative Large Language Models. *arXiv* **2024**, arXiv:2411.18530.
19. Asaad, A.; Ali, D.; Majeed, T.; Rashid, R. Persistent homology for breast tumor classification using mammogram scans. *Mathematics* **2022**, *10*, 4039. [CrossRef]
20. Maršálek, R.; Zedka, R.; Zöchmann, E.; Vychodil, J.; Závorka, R.; Ghiaasi, G.; Blumenstein, J. Persistent homology approach for human presence detection from 60 GHz OTFS transmissions. *Sensors* **2023**, *23*, 2224. [CrossRef]
21. Branco, S.; Carvalho, J.G.; Reis, M.S.; Lopes, N.V.; Cabral, J. 0-Dimensional Persistent Homology Analysis Implementation in Resource-Scarce Embedded Systems. *Sensors* **2022**, *22*, 3657. [CrossRef]
22. Malek, A.A.; Alias, M.A.; Razak, F.A.; Noorani, M.S.M.; Mahmud, R.; Zulkepli, N.F.S. Persistent Homology-Based Machine Learning Method for Filtering and Classifying Mammographic Microcalcification Images in Early Cancer Detection. *Cancers* **2023**, *15*, 2606. [CrossRef]
23. Choe, S.; Ramanna, S. Cubical homology-based machine learning: An application in image classification. *Axioms* **2022**, *11*, 112. [CrossRef]
24. Wang, X.; Yuan, B.; Li, Z.; Wang, H. A Fractal Curve-Inspired Framework for Enhanced Semantic Segmentation of Remote Sensing Images. *Sensors* **2024**, *24*, 7159. [CrossRef]
25. Ji, Z.; Ziyu, L.; Angsheng, W.; Peng, C. An approach to extracting fractal in remote sensing image. *Wuhan Univ. J. Nat. Sci.* **2006**, *11*, 606–610. [CrossRef]
26. Sun, W.; Xu, G.; Gong, P.; Liang, S. Fractal analysis of remotely sensed images: A review of methods and applications. *Int. J. Remote Sens.* **2006**, *27*, 4963–4990. [CrossRef]
27. Kato, C.N.; Barra, S.G.; Tavares, N.P.; Amaral, T.M.; Brasileiro, C.B.; Mesquita, R.A.; Abreu, L.G. Use of fractal analysis in dental images: A systematic review. *Dentomaxillofac. Radiol.* **2020**, *49*, 20180457. [CrossRef] [PubMed]
28. Huang, J.; Zhou, Y.; Luo, Y.; Liu, G.; Guo, H.; Yang, G. Representing Topological Self-Similarity Using Fractal Feature Maps for Accurate Segmentation of Tubular Structures. In Proceedings of the 18th European Conference on Computer Vision, Milan, Italy, 29 September–4 October 2024; pp. 143–160.
29. Wasserman, L. Topological data analysis. *Annu. Rev. Stat. Appl.* **2018**, *5*, 501–532. [CrossRef]
30. Abdullahi, M.S.; Suratanee, A.; Piro, R.M.; Plaimas, K. Persistent Homology Identifies Pathways Associated with Hepatocellular Carcinoma from Peripheral Blood Samples. *Mathematics* **2024**, *12*, 725. [CrossRef]
31. Esser, P.; Kulal, S.; Blattmann, A.; Entezari, R.; Müller, J.; Saini, H.; Levi, Y.; Lorenz, D.; Sauer, A.; Boesel, F.; et al. Scaling rectified flow transformers for high-resolution image synthesis. In Proceedings of the Forty-First International Conference on Machine Learning, Vienna, Austria, 21–27 July 2024.
32. Cohen-Steiner, D.; Edelsbrunner, H.; Harer, J. Stability of Persistence Diagrams. *Discret. Comput. Geom.* **2005**, *37*, 103–120. [CrossRef]
33. Cohen-Steiner, D.; Edelsbrunner, H.; Harer, J.; Mileyko, Y. Lipschitz Functions Have Lp-Stable Persistence. *Found. Comput. Math.* **2010**, *10*, 127–139. [CrossRef]
34. Patel, A. Generalized persistence diagrams. *J. Appl. Comput. Topol.* **2016**, *1*, 397–419. [CrossRef]
35. Clough, J.; Byrne, N.; Oksuz, I.; Zimmer, V.; Schnabel, J.; King, A. A Topological Loss Function for Deep-Learning Based Image Segmentation Using Persistent Homology. *IEEE Trans. Pattern Anal. Mach. Intell.* **2019**, *44*, 8766–8778. [CrossRef]
36. Mandelbrot, B.B.; Van Ness, J.W. Fractional Brownian Motions, Fractional Noises and Applications. *SIAM Rev.* **1968**, *10*, 422–437. [CrossRef]
37. la Torre, F.L.; GonzÃ¡lez-Trejo, J.; Real-RamÃ rez, C.; Hoyos-Reyes, L.F. Fractal dimension algorithms and their application to time series associated with natural phenomena. *J. Phys. Conf. Ser.* **2013**, *475*, 012002. [CrossRef]

38. Podell, D.; English, Z.; Lacey, K.; Blattmann, A.; Dockhorn, T.; Muller, J.; Penna, J.; Rombach, R. SDXL: Improving Latent Diffusion Models for High-Resolution Image Synthesis. *arXiv* **2023**, arXiv:2307.01952.
39. Blattmann, A.; Dockhorn, T.; Kulal, S.; Mendelevitch, D.; Kilian, M.; Lorenz, D. Stable Video Diffusion: Scaling Latent Video Diffusion Models to Large Datasets. *arXiv* **2023**, arXiv:2311.15127.
40. Xie, E.; Chen, J.; Chen, J.; Cai, H.; Lin, Y.; Zhang, Z.; Li, M.; Lu, Y.; Han, S. SANA: Efficient High-Resolution Image Synthesis with Linear Diffusion Transformers. *arXiv* **2024**, arXiv:2410.10629.
41. Gu, J.; Zhai, S.; Zhang, Y.; Susskind, J.M.; Jaitly, N. Matryoshka Diffusion Models. *arXiv* **2023**, arXiv:2310.15111.
42. Yao, F.; Zhang, H.; Gong, Y. Difsg2-ccl: Image reconstruction based on special optical properties of water body. *IEEE Photonics Technol. Lett.* **2024**, *36*, 1417–1420. [CrossRef]
43. Wang, Z.; Chen, M.; Guo, Y.; Li, Z.; Yu, Q. Bridging the domain gap in satellite pose estimation: A self-training approach based on geometrical constraints. *IEEE Trans. Aerosp. Electron. Syst.* **2023**, *60*, 2500–2514. [CrossRef]
44. Horak, D.; Yu, S.; Salimi-Khorshidi, G. Topology distance: A topology-based approach for evaluating generative adversarial networks. *Proc. AAAI Conf. Artif. Intell.* **2021**, *35*, 7721–7728. [CrossRef]
45. Alipourjeddi, N.; Miri, A. Evaluating Generative Adversarial Networks: A Topological Approach. In Proceedings of the 2023 International Conference on Computing, Networking and Communications (ICNC), Honolulu, HI, USA, 20–22 February 2023; pp. 202–206.